

Extreme electron-phonon coupling in boron-based layered superconductors

J. M. An,¹ S. Y. Savrasov,² H. Rosner,³ and W. E. Pickett³

¹Lawrence Berkeley National Laboratory, Berkeley, California 94720

²Department of Physics, New Jersey Institute of Technology, Newark, New Jersey 07102

³Department of Physics, University of California, Davis, California 95616

(Received 11 October 2002; published 31 December 2002)

The phonon-mode decomposition of the electron-phonon coupling in the MgB₂-like system Li_{1-x}BC is explored using first-principles calculations. It is found that the high-temperature superconductivity of such systems results from extremely strong coupling up to only ~2% of the phonon modes. Noteworthy characteristics of E_{2g} branches include (1) “mode λ” values of 25 and greater compared to a mean of ~0.4 for other modes, (2) a precipitous Kohn anomaly, and (3) E_{2g} phonon linewidths within a factor of ~2 of the frequency itself, indicating impending breakdown of conventional electron-phonon theory. This behavior is borne out by recent inelastic x-ray scattering studies of MgB₂ by Shukla *et al.*

DOI: 10.1103/PhysRevB.66.220502

PACS number(s): 74.25.Jb, 74.25.Kc, 74.70.Ad

Superconductivity near $T_c \approx 40$ K in MgB₂¹ has necessitated a reevaluation of our understanding of phonon-coupled superconductivity, and illustrated vividly that there has been a substantial void in our conceptual understanding of this “conventional” mechanism of coupling, long thought to require d electrons, high density of states, and high symmetry. The general theory of electron-phonon (EP) coupled superconductivity has long been available,^{2,3} and some essential understanding of the mechanism in MgB₂ is now in place.^{4–10} The particular structure and chemistry of MgB₂ creates holes in the B $2p\sigma$ bands, and these holes are coupled very strongly to the B-B bond-stretching vibrational modes. The predictions of band theory have been verified by angle-resolved photoemission¹¹ and de Haas–van Alphen measurements.^{12–14} One unexpected facet is an unusually strong anisotropy in the EP coupling, such that the Fermi-surface (FS) averaged EP coupling strength λ and Eliashberg function $\alpha^2F(\omega)$ do not give a precise account of T_c or of thermal and spectroscopic data. It seems, however, that much can be accounted for by generalizing to a two-band model^{9,10} of strongly coupled σ holes and weakly coupled π electrons, with $\lambda = \lambda_\sigma + \lambda_\pi \approx 0.6 - 0.8$.

In spite of the success in accounting for many observations, this linear EP theory (with some *ad hoc* correction for anharmonicity) seems at best incomplete. The enormous linewidth γ of the E_{2g} mode,^{15–18} ascribed to strong EP coupling plus anharmonicity, has not been accounted for quantitatively, and the predicted change in frequency and γ at T_c ⁹ is not observed. Nonadiabatic processes arising from the small filling of the σ bands, and low Fermi energy E_F , have been proposed.^{9,19,20} Boeri *et al.* provided needed clarification by demonstrating that E_{2g} anharmonicity arises in MgB₂ from nonadiabatic effects,²¹ due to the huge deformation potential.⁴

A second compound in the “MgB₂ class” that has been proposed recently is useful in clarifying these issues. LiBC is isostructural²² and isovalent with MgB₂, having graphene-like B-C layers that are even more strongly bonded than are the B layers of MgB₂. The stoichiometric compound is semiconducting (due to the B-C difference), but Li deficiency that makes it a hole-doped metal has been reported.²² Such hole

doping introduces carriers into the B-C σ bands, as occurs in MgB₂, and near rigid-band behavior has been demonstrated, making it a promising system for probing the carrier density dependence of EP coupling in MgB₂-class superconductors.

In this paper, we focus on the decomposition of λ into contributions (“mode λ’s”) from each phonon $Q\nu$ rather than its FS decomposition, and find startlingly high values $\lambda_{Q\nu} \approx 25$ for E_{2g} modes. First-principles calculations of α^2F for Li_{0.75}BC gives $\lambda = 0.74$, making Li_{1-x}BC at this doping level quantitatively similar to MgB₂. The insulating end member of the Li_{1-x}BC system makes it pedagogically an ideal material to illustrate the distinct aspects that MgB₂ has introduced into the physics of electron-phonon coupled superconductivity. Li_{1-x}BC is “MgB₂ with stronger coupling and variable carrier concentration,” and because its σ FS’s are (as in MgB₂) very close to cylindrical, the underlying physical processes can be modeled simply yet realistically. The essential revelations are: (1) the high-temperature superconductivity arises from exceedingly strong coupling of only a small fraction (~2%, depending on doping) of the phonon modes, (2) a colossal sharp Kohn anomaly occurs—extreme renormalization by EP coupling upon doping from hard bond-stretching modes, and (3) the phonon linewidth due to decay into σ band electron-hole pairs becomes comparable to the linewidth itself, making the bond-stretching modes poorly defined (at best), yet not unstable (due to their intrinsic hard nature). Just this strength of coupling and relative linewidths have been reported for MgB₂ by Shukla *et al.*, obtained from inelastic x-ray scattering spectroscopy.²³ Moreover, (4) these effects occur continuously with doping and will allow a unique window into the nonadiabatic regime, where the Fermi energy is comparable to the phonon frequency. These features apply directly to Mg_{1-x}Al_xB₂ as well.

A description of the band structure of Li_{1-x}BC was presented earlier.²⁴ The FS’s for $x = 0.25$, pictured in Fig. 1, consist of four B(2p)–C(2p) σ band cylinders with very small k_z dispersion, and a π band FS. The σ cylinders are similar to those in MgB₂, with four cylinders (instead of the two in MgB₂) arising from the doubling of the unit cell

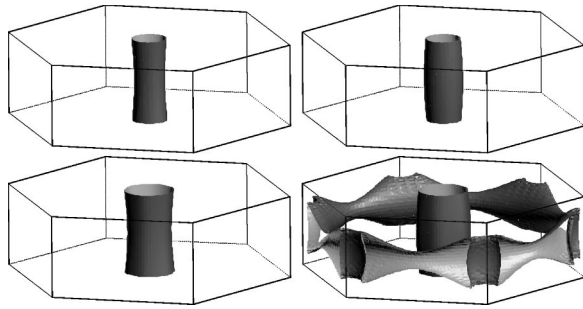


FIG. 1. Fermi surfaces of $\text{Li}_{0.75}\text{BC}$, with the Γ point at the center of the hexagonal zone. There are four cylinders, analogous to the two cylinders in MgB_2 but downfolded due to the doubled unit cell. The noncylindrical surface arises from the weakly coupled π bands.

along c due to alternate stacking of B-C layers. The phonon energies and EP matrix elements have been obtained from linear-response theory,²⁵ as implemented in Savrasov's full-potential linear muffin-tin-orbital code.^{26,27} Because of the emphasis here on specific Fermi-surface effects, a dense grid of Q points was chosen (a 16,16,4 grid giving 90 Q points in the irreducible wedge). For k -space integration, a finer 32,32,8 grid was used, together with an adaptive tetrahedron integration scheme.²⁶ The code was used previously for MgB_2 by Andersen's group,⁶ where the need for careful zone sampling was also emphasized.

For the semiconducting phase, the E_{2g} phonons (Fig. 2) are very hard, lying at 150 meV at the Γ point and not dispersing greatly. This high bond-stretching frequency, twice as high as in MgB_2 , is due to the much stronger B—C bond, 9% shorter and having a 40% larger deformation potential for the σ bands.²⁴ The spectrum is indicative of a stable, strongly bonded material. For $x=0.25$, where it has become a metal (Fig. 2), there is rather a little difference in the spectra, *except* for $Q_{\parallel} < 2k_F \approx \pi/3a$ (Q_{\parallel} is the component of the phonon wave vector \vec{Q} lying in the plane). Within this region, however, the four E_{2g} -related modes display a precipitous Kohn anomaly at $2k_F$, and dip *nearly discontinuously* by 40%. (The decrease in ω^2 , which directly reflects the renormalization, is nearly 65%). Closely related renormalization of phonon modes in the $\text{Mg}_{1-x}\text{Al}_x\text{B}_2$ system has been noted by Renker *et al.*²⁸

In Fig. 3, the phonon density of states (DOS) for $x=0$ and $x=0.25$ are contrasted, and also the calculated EP spectral function $\alpha^2F(\omega)$ for $x=0.25$ is compared with the DOS. For the DOS, doping moves the modes in the frequency range 135–155 meV to lower frequency; only from the dispersion curves of Fig. 2 is it clear where they end up (in the 85 meV region) because these modes are near the Γ point where phase space is small. The curve for $\alpha^2F(\omega)$ demonstrates what results: a tiny fraction of modes (quantified below) in the 85 meV region are extremely strongly coupled to the σ band holes, and leads to an inordinately strong contribution to λ , whose total value calculated from α^2F is 0.74. Although about half of the coupling arises from all other modes, it is the extremely strong coupling of small- Q E_{2g} modes to σ holes that drives T_c , just as in MgB_2 . The cal-

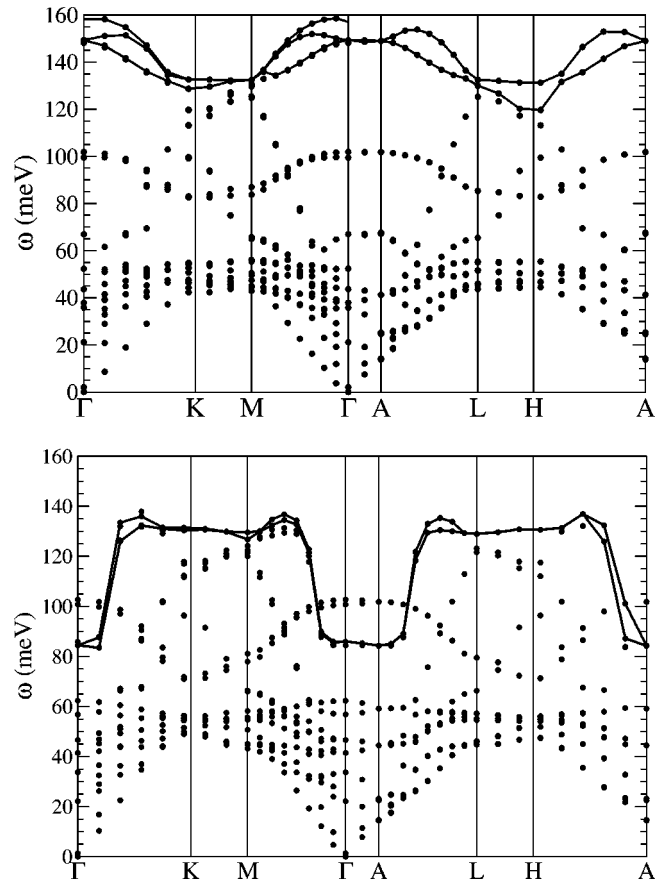


FIG. 2. Calculated phonon dispersion curves for (top) semiconducting LiBC and (bottom) strongly hole-doped and metallic $\text{Li}_{0.75}\text{BC}$, with E_{2g} -derived modes connected by heavy lines. The primary difference is the extremely strong renormalization downward (ω_D^2 decreases by $\sim 60\%$) for $Q < 2k_F$; the extreme van Hove singularities along $\Gamma-K$, $M-\Gamma$, $A-L$, $H-A$ are apparent.

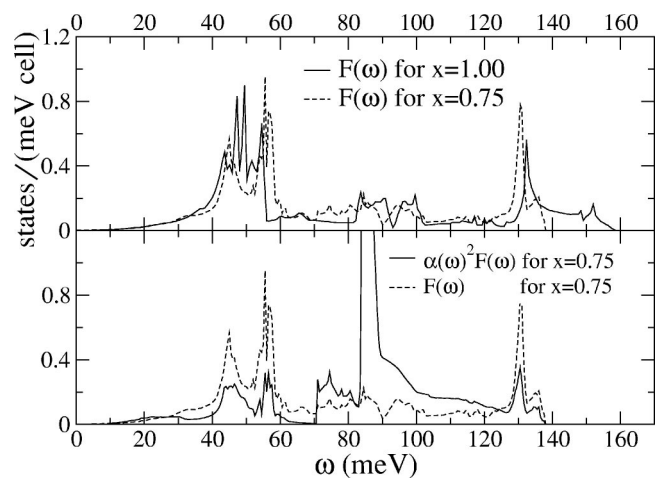


FIG. 3. Phonon DOS for LiBC and $\text{Li}_{0.75}\text{BC}$ (top panel) where the primary difference is the disappearance of modes in the range 135–155 meV upon doping (from Fig. 1, they mostly lie in the 80–90 meV region). The shape of $F(\omega)$ and $\alpha^2F(\omega)$ for $\text{Li}_{0.75}\text{BC}$ (bottom panel) revealing the extremely strong coupling to phonons in the 85–100 meV range.

culated value of T_c using the Allen-Dynes equation²⁹ is 34 K assuming $\mu^* = 0.09$ as has been used previously¹⁰ to obtain a numerical agreement with the observed T_c for MgB₂. Solution of the anisotropic Eliashberg equations¹⁰ would give T_c several degrees higher.

The circular σ Fermi surfaces of MgB₂ and related materials allow an analytic treatment of EP coupling. The phonon energies ($\hbar = 1$) are given by the poles of the lattice Green's function,

$$\omega_{Q\nu}^2 = \Omega_{Q\nu}^2 + 2\Omega_{Q\nu}\Pi^\sigma(Q, \omega_{Q\nu}), \quad (1)$$

where the reference frequency $\Omega_{Q\nu}$ includes all self-energy effects except those arising from electron scattering within the σ bands; practically speaking, they are the energies shown in Fig. 2 for undoped LiBC. Taking for simplicity a single cylindrical Fermi surface with $N(\varepsilon) = m^*/2\pi$ per spin per unit area, and considering the E_{2g} derived modes only, the phonon self-energy due to the σ carriers is ($\eta_Q \equiv Q_{\parallel}/2k_F$)

$$\Pi^\sigma(Q, \omega) = -2 \sum_k |M_{k,Q}|^2 \frac{f_k - f_{k+Q}}{\varepsilon_{k+Q} - \varepsilon_k - \omega - i\delta},$$

$$\text{Re } \Pi^\sigma(Q, \omega_Q) \approx -2 |M_{2g}|^2 N(\varepsilon_F) \hat{\chi}_L^{2D}(Q), \quad (2)$$

$$\hat{\chi}_L^{2D}(Q) = \theta(1 - \eta_Q) + [1 - \sqrt{1 - \eta_Q^2}] \theta(\eta_Q - 1). \quad (3)$$

Here, $f_k \equiv f(\varepsilon_k)$ is the Fermi occupation factor, and the usual adiabatic approximation has been made. A mean-square matrix element has been extracted from the sum, leaving the unitless Lindhard function $\hat{\chi}_L^{2D}$.³⁰ The negative of $\hat{\chi}_L^{2D}(Q)$ has much the form that is evident in the softened E_{2g} branches with $Q < 2k_F$ in the bottom panel of Fig. 2. This behavior is illustrated by plotting ω_Q given by Eqs. (1)–(3) in the bottom panel of Fig. 4.

The ‘‘mode λ ’’ $\lambda_{Q\nu}$ ³¹ for the E_{2g} modes, defined such that it is an intensive quantity whose average over the zone and over the N_ν branches gives λ_{2g} ($\lambda = \lambda_{2g} + \lambda_{other}$), is

$$\lambda_{\tilde{Q}} = \frac{2N_\nu}{\pi N(\varepsilon_F)} \frac{\gamma_Q}{\omega_Q^2}, \quad \gamma_Q = \pi \Omega_Q |M_{2g}|^2 \xi(Q),$$

$$\xi(Q) = \sum_k \delta(\varepsilon_k) \delta(\varepsilon_{k+Q}) \equiv N(0)^2 \frac{A_{BZ}}{A_{FS}} \frac{\hat{\xi}(Q/2k_F)}{\pi}, \quad (4)$$

where $\hat{\xi}(\eta) = \eta^{-1}(1 - \eta^2)^{-1/2} \theta(\eta) \theta(1 - \eta)$. Here, A_{BZ} , is the basal area of the Brillouin zone (BZ) and $A_{FS} = \pi(2k_F)^2$ is a doping-dependent area of renormalized E_{2g} phonons. $Q \rightarrow 0$ requires somewhat more care³² but involves negligible phase space for the present purposes. The important feature, aside from the magnitude, is that these mode λ 's scale inversely with k_F^2 as illustrated in Fig. 4, diverging for vanishing σ hole doping and indicating the breakdown of conventional EP theory (see below).

For $Q < 2k_F$, ω_Q and Ω_Q are nearly constant, so Eqs. (1) and (2) can be solved for $|M_{2g}|^2$ and substituted into Eq. (4) to provide a simple expression for the mode λ_Q ($Q < 2k_F$) in

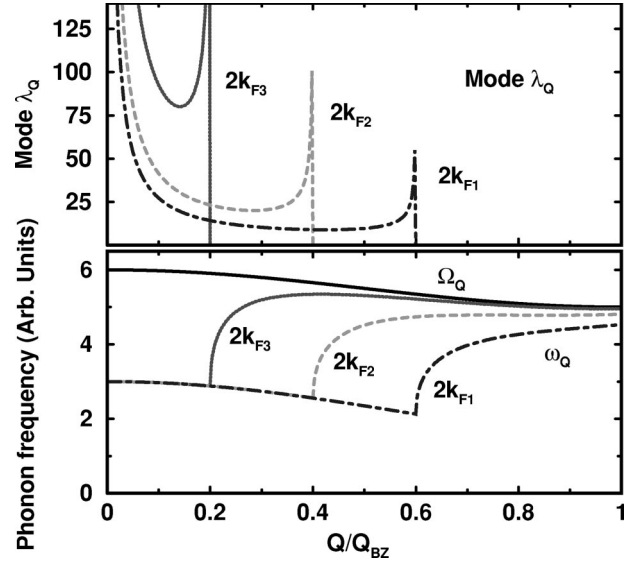


FIG. 4. Characteristics of the 2D (two-dimensional) electrons (see text) strongly coupled to E_{2g} modes. Bottom panel: E_{2g} branch versus Q ; reference branch Ω_Q and renormalized branch ω_Q as in Eqs. (1)–(3), for three different values of $2k_F$. Top panel: Corresponding values of the mode λ_Q given by Eq. 4, for the same three values of $2k_F$.

terms of $(\Omega_{2g}^2 - \omega_{2g}^2)/\omega_{2g}^2$. Similar expression have been used for Nb-Mo alloys³³ and for Pb alloys³⁴ to relate λ to phonon softening. There is a simpler way to obtain the average mode λ for E_{2g} phonons. The total contribution is that obtained from the 85–100 meV region (see Fig. 3) of α^2F , $\lambda_{2g} = 0.4$. This arises from an average over all phonons, but only those in 3/40 of the BZ ($Q < 2k_F$) and the upper four of 18 of the branches contribute. Hence, the mean is $\langle \lambda_Q^{2g} \rangle = 0.4 \times (40/3) \times (18/4) \approx 25$. The full Q dependence of the mode λ_Q for the E_{2g} branches is given by Eq. (4) and shown in the top panel of Fig. 4. The mean mode λ from all other phonons (equal to their contribution to λ since it includes 98% of all modes) also is $\lambda_{other} \approx 0.4$, accounting for the total $\lambda = 0.74$ obtained from α^2F .

The phonon relative half-width³¹ becomes $\gamma_Q/\omega_Q \sim 0.5\lambda_Q/(\lambda_{2g}) \sim 0.5$, an alarming result (this ratio is typically 10^{-2} – 10^{-3}) that reflects the fact that this phonon branch is so ill defined from the extremely strong EP coupling such that the Migdal theory (and the Eliashberg theory) is no longer justified. Even so, this rough estimate is consistent with the large observed half-width^{15–18} of 125 – 175 cm^{-1} for the 600 cm^{-1} bond-stretching mode, indicating that the large linewidth and its strong increase with temperature is due to EP coupling rather than due to anharmonicity, and the same conclusion has been reached by Shukla *et al.*²³

Now, we summarize and discuss some implications of these results. Use of Li_{1-x}BC has allowed us to identify and quantify the drastic phonon softening arising from the ultrastrong EP coupling to E_{2g} modes; comparable phenomena occur also in MgB₂. Mode λ_{2g} 's ≈ 25 and linewidths comparable to the frequency point to inadequacies of conventional EP theory for these systems. Shukla *et al.* have

reported²³ measurements of specific frequencies and line-widths of MgB_2 from inelastic x-ray scattering. For five small- Q_{\parallel} E_{2g} phonons with frequencies in the 500–550 cm^{-1} range, they obtained relative linewidths $\gamma_Q/\omega_Q \approx 1/3$, very consistent with our results above. For these modes, the average $\lambda_Q = 26$ (when normalized as we have done) are again exactly in line with the expectations outlined above.

This extremely strong and abruptly Q -dependent EP coupling provides a different insight into the relationship of limits on T_c and lattice instability.³⁵ A previous study had produced both the arguments that the incipient lattice instabilities are helpful^{33,34} for T_c , and that they are unhelpful because the low-frequency modes are less useful for high T_c than higher frequencies (of the order of $2\pi T_c$).³⁶ The lack of explicit dependence of λ_{2g} on k_F indicates that the increase in T_c with doping will arise only from an increase of m^* (the heavy hole mass increases by 25% from $x=0$ to $x=0.5$) or

increase of $|M_{2g}|^2$, either of which will further soften the E_{2g} modes and move the system closer to instability. What changes rapidly with doping is the coupling *strength* of the E_{2g} modes with $Q < 2k_F$ —the same total EP coupling strength is concentrated into increasingly fewer bond-stretching modes at lower doping levels. Thus, in this system (where the two dimensionality of the electron dispersion is central), change of the doping level can lead to large redistributions of coupling strength without any direct effect on T_c itself. These features, arising from extremely strong coupling, apply to $\text{Mg}_{1-x}\text{Al}_x\text{B}_2$, where unexplained structural anomalies occur, as well as to Li_{1-x}BC .

W.E.P. acknowledges important discussions with I. I. Mazin and O. K. Andersen related to mode λ 's in MgB_2 . This work was supported by National Science Foundation Grant No. DMR-0114818, and by the Deutscher Akademischer Austauschdienst.

-
- ¹J. Nagamatsu *et al.*, Nature (London) **410**, 63 (2001).
²D.J. Scalapino, J.R. Schrieffer, and J.W. Wilkins, Phys. Rev. **148**, 263 (1966).
³P. B. Allen and B. Mitrović, in *Solid State Physics* (Academic, New York, 1982), Vol. 37, pp. 2-92; P. B. Allen, in *Dynamical Properties of Solids*, edited by G. K. Horton and A. A. Maradudin (North-Holland, Amsterdam, 1980), Chap. 2.
⁴J.M. An and W.E. Pickett, Phys. Rev. Lett. **86**, 4366 (2001)
⁵J. Kortus *et al.*, Phys. Rev. Lett. **86**, 4656 (2001).
⁶Y. Kong *et al.*, Phys. Rev. B **64**, 020501 (2001).
⁷K.-P. Bohnen, R. Heid, and B. Renker, Phys. Rev. Lett. **86**, 5771 (2001).
⁸T. Yildirim *et al.*, Phys. Rev. Lett. **87**, 037001 (2001).
⁹A.Y. Liu, I.I. Mazin, and J. Kortus, Phys. Rev. Lett. **87**, 087005 (2001).
¹⁰H.J. Choi *et al.*, Phys. Rev. B **66**, 020513(R) (2002).
¹¹H. Uchiyama *et al.*, Phys. Rev. Lett. **88**, 157002 (2002).
¹²E.A. Yelland *et al.*, Phys. Rev. Lett. **88**, 217002 (2002).
¹³I.I. Mazin and J. Kortus, Phys. Rev. B **65**, 180510 (2002).
¹⁴H. Rosner *et al.*, Phys. Rev. B **66**, 024521 (2002).
¹⁵J. Hlinka *et al.*, Phys. Rev. B **64**, 140503 (2001).
¹⁶H. Martinho *et al.*, cond-mat/0105204 (unpublished).
¹⁷J.W. Quilty *et al.*, Phys. Rev. Lett. **88**, 087001 (2002).
¹⁸P. M. Rafailov *et al.*, Solid State Commun. **122**, 455 (2002).
¹⁹E. Cappelluti *et al.*, Phys. Rev. Lett. **88**, 117003 (2002).
²⁰Y.-W. Son, J. Yu, and J. Ihm, cond-mat/0203204 (unpublished).
²¹L. Boeri *et al.*, Phys. Rev. B **65**, 214501 (2002).
²²M. Wörle *et al.*, Z. Anorg. Allg. Chem. **621**, 1153 (1995).
²³A. Shukla *et al.*, cond-mat/0209064 (unpublished).
²⁴H. Rosner, A. Kitaigorodsky, and W.E. Pickett, Phys. Rev. Lett. **88**, 127001 (2002).
²⁵S. Baroni, S. de Gironcoli, and A. Dal Corso, Rev. Mod. Phys. **73**, 515 (2001).
²⁶S.Y. Savrasov, Phys. Rev. B **54**, 16 470 (1996); S.Y. Savrasov and D.Y. Savrasov, *ibid.* **54**, 16 487 (1996).
²⁷O.K. Andersen and O. Jepsen, Phys. Rev. Lett. **53**, 2571 (1984).
²⁸B. Renker *et al.*, Phys. Rev. Lett. **88**, 067001 (2002).
²⁹P.B. Allen and R.C. Dynes, Phys. Rev. B **12**, 905 (1975).
³⁰J.G. Kim *et al.*, Phys. Rev. B **59**, 3661 (1999).
³¹P.B. Allen, Phys. Rev. B **6**, 2577 (1972); P.B. Allen and M.L. Cohen, Phys. Rev. Lett. **29**, 1593 (1972).
³²C.O. Rodriguez *et al.*, Phys. Rev. B **42**, 2692 (1990).
³³W.E. Pickett and P.B. Allen, Phys. Rev. B **16**, 3127 (1977).
³⁴P.B. Allen and R.C. Dynes, Phys. Rev. B **11**, 1895 (1975).
³⁵M. L. Cohen and P. W. Anderson, in *Superconductivity in d- and f-Band Metals*, edited by D. H. Douglass (AIP, New York, 1972); D.A. Kirzhnits *et al.*, J. Low Temp. Phys. **10**, 79 (1973); P.B. Allen, M.L. Cohen, and D.R. Penn, Phys. Rev. B **38**, 2513 (1988).
³⁶G. Bergmann and D. Rainer, Z. Phys. A **263**, 59 (1973).